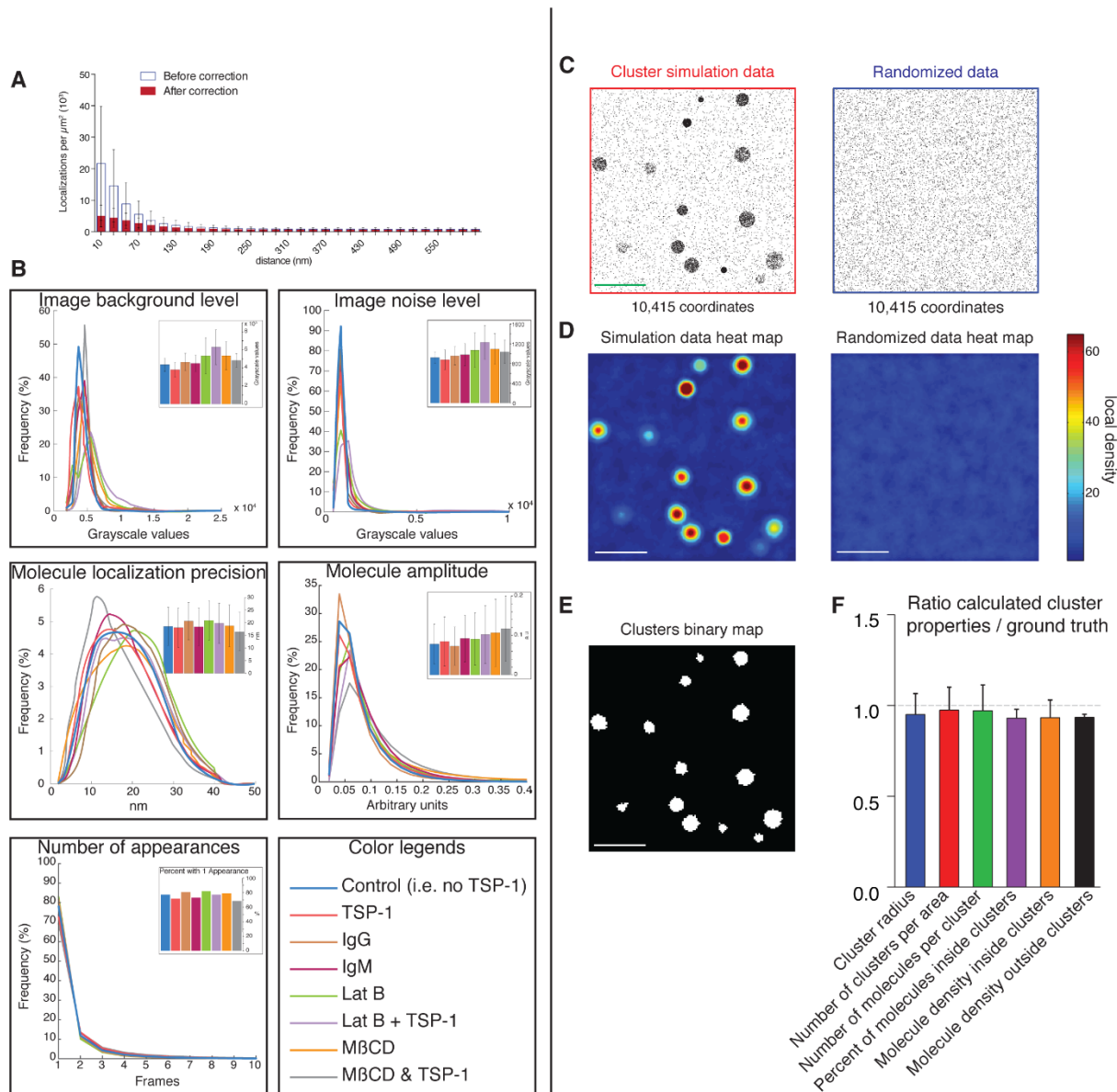


**Fig S1. CD36, Fyn and Src expression controls and TSP-1 binding controls for experiments shown in Fig 1.**

(A) Projection of z-stacks of confocal images of surface CD36 expression in pHMVECs, HMEC-1 and HMEC-CD36-myc cells, and total CD36 expression in HMEC-mApple-CD36. Cell nuclei stained with DAPI (blue). Surface receptors in pHMVECs, HMEC-1 and HMEC-CD36-myc were labeled using primary mouse anti-human CD36 (FA6-152) and secondary donkey anti-mouse Cy3. Scale bars, 5  $\mu\text{m}$ . (B-C) Flow cytometry analysis of CD36 expression in engineered HMEC cells compared to low passage number pHMVECs (because pHMVECs lose CD36 over time). Indicated cells were fixed and stained using mouse anti-CD36 (clone FA6-152) and secondary donkey anti-mouse AlexaFluor-647 antibodies. The fraction of cells expressing CD36 (B) was determined by gating positive cells (with a fluorescence signal higher than the threshold defined by the isotype control staining) from the whole cell population and converted to a percentage. Data are means  $\pm$  SD determined from 3 independent experiments. Fold expression of CD36 (C) was measured as the mean fluorescence intensity of CD36 positive cells normalized to the mean level in pHMVEC cells. Data as for (B). (D) Projection of z-stacks of confocal images of TSP-1-Cy3b bound to pHMVECs (15 min incubation) treated with non-specific siRNA (NS siRNA) or CD36 siRNA. Cells were fixed and stained for surface CD36 using mouse anti-human CD36 (FA6-152) and secondary donkey anti-mouse AlexaFluor-488 antibodies. Nuclei were labeled with DAPI. Insets represent magnified areas indicated by dashed line boxes. Scale bars, 5  $\mu\text{m}$ . (E) Levels of TSP-1 binding were determined as the mean TSP-1-Cy3b intensity within cells (segmented based on DIC image) and normalized to the mean of the NS siRNA condition. 30 data points from 3 independent experiments were analyzed. Error bars indicate SD. Comparison p-value obtained using Student's t-test. Black line indicates p-value  $< 0.05$ . (F) Western blot of cell lysates prepared from HMEC-mApple-CD36 cells treated or not with non-specific, Fyn siRNA or Src siRNA, with rabbit anti-Fyn or rabbit anti-Src and secondary donkey anti-rabbit HRP antibodies. Tubulin was used as loading control by simultaneous immunoblotting with mouse anti-tubulin and secondary donkey anti-mouse Cy3 antibodies. (G) Percentage of Src and Fyn expression normalized to the untreated value and quantified from blots in (F). Error bars show SD. Pair-wise comparison p-values obtained using Student's t-test. Black lines indicate p-value  $< 0.05$ .



**Fig S2. Assessment of PALM data, including comparison of image and data quality measures between conditions, and validation of SPA.**

(A) Histograms of absolute densities of localization before (empty histogram with blue outline) and after (red histogram) multi-appearance correction of CD36 coordinates, calculated using the pair-correlation function (Materials & Methods). Data from 21 movies. Error bars indicate SD. (B) PALM image (top row) and localization (middle and bottom rows) quality measures for all conditions in our study. Main panels show full distributions. Insets show mean and standard deviation of each distribution, except for “number of appearances” inset which shows percentage of molecules with only 1 appearance. (C-F) Validation of SPA (Materials & Methods). (C) Instance of a field of simulated clusters (red ROI) and randomization of equal number of coordinates within an ROI of same size (blue ROI). Scale bar, 1  $\mu\text{m}$  (in Panels C-E). (D) Cluster heat maps of simulation in (C) (left) and its randomized control (right). Pseudo-colors indicate local density values at radius of 50 nm. (E) Binary map of clusters detected in simulated data in (C) using the threshold derived from the randomization control. (F) Ratio of cluster properties calculated from the thresholded clusters to the simulation ground truth properties. The graph represents results from 150 heterogeneous simulations with varying number of clusters per area, number of molecules per cluster, percent of molecules in clusters, and cluster radius. Error bars indicate SD.

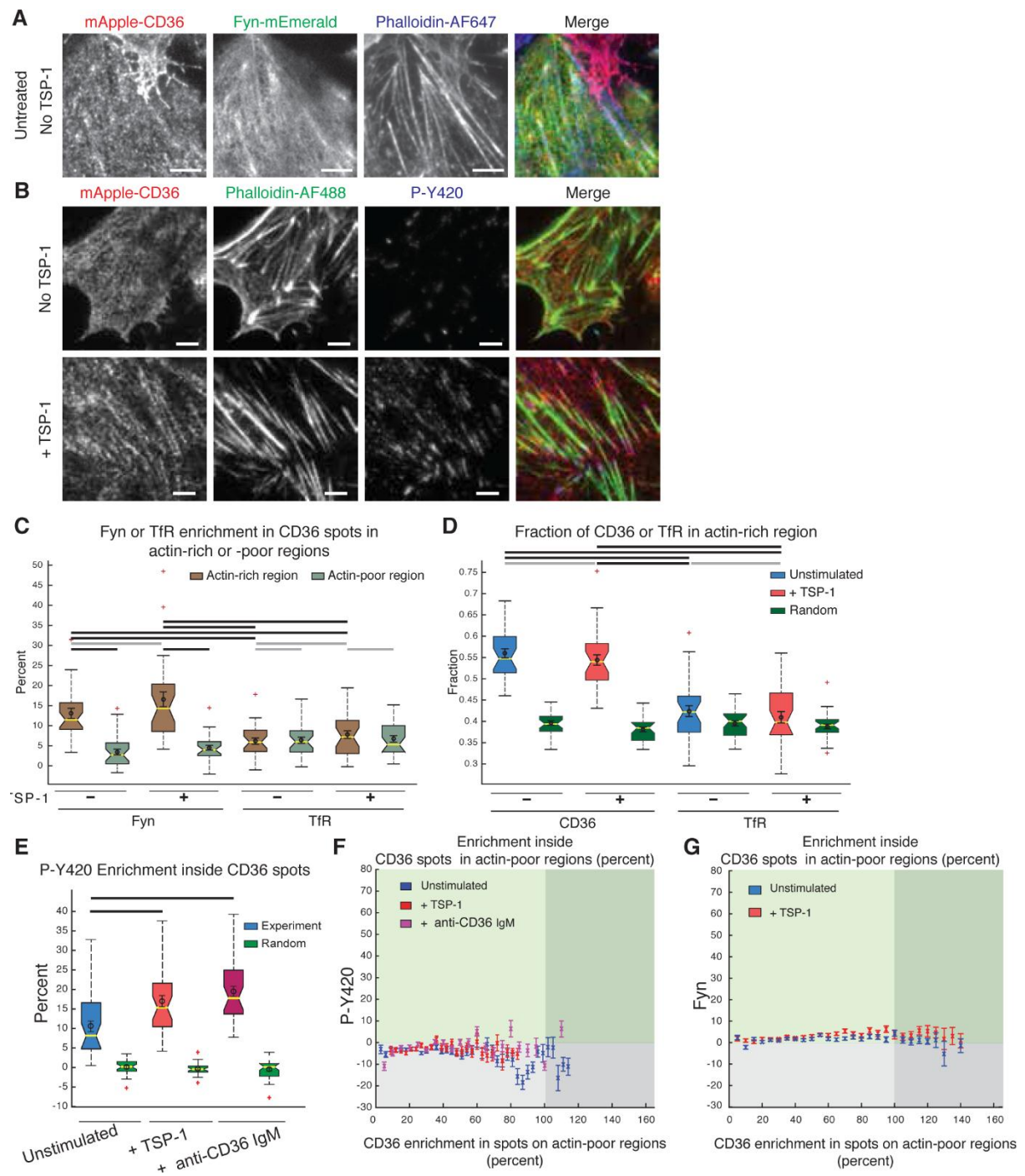


**Fig S3. Fyn, P-Y420 or transferrin receptor (TfR) enrichment at CD36 clusters in actin-rich and -poor regions.**

(A) TIRFM of WT Fyn-mEmerald transfected in HMEC-mApple-CD36 cells also labeled for F-actin with phalloidin-AlexaFluor-647. Scale bars, 5  $\mu\text{m}$ . (B) TIRFM of HMEC-mApple-CD36 cells stimulated or not with 10 nM TSP-1 for 10 min and labeled for F-actin (phalloidin-AlexaFluor-488) and P-Y420 using anti-PY420 primary and Dylight649 coupled secondary antibodies. Scale bars, 5  $\mu\text{m}$ . (C) HMEC-mApple-CD36 cells transfected with Fyn-mEmerald or an unrelated membrane receptor TfR-GFP were stimulated or not for 10 min with 10 nM TSP-1, fixed and stained for F-actin using phalloidin-AlexaFluor-647 and imaged by TIRFM. Fyn-mEmerald or TfR enrichment within mApple-CD36 spots in actin rich or poor regions (Fyn part of (C) is a repeat of Fig 3I). Boxplots and statistical tests as in Fig 1E (for 10 comparisons, significance threshold = 0.0051 for each comparison). Data from > 30 fields of view from 3 independent experiments, all imaged with identical settings. (D) The fraction of mApple-CD36 or TfR-GFP spots in actin-rich regions (from experiments described in (C)) was compared to randomized control (green boxes). Boxplots and statistical tests as (C) (for 6 comparisons, significance threshold = 0.0085 for each comparison). (E) P-Y420 enrichment at CD36 spots without distinguishing between actin rich or poor regions (shown in Fig 4D), compared to randomized control. Boxplots and statistical tests as in Fig 1E (for 2 comparisons, significance threshold = 0.025 for each comparison). (F) Scatter plot of P-Y420 enrichment vs. CD36 enrichment within mApple-CD36 spots similar to Fig 4E but for actin-poor regions. (G) Scatter plot of Fyn-mEmerald enrichment vs. CD36 enrichment within mApple-CD36 spots similar to Fig 4F but for actin-poor regions.

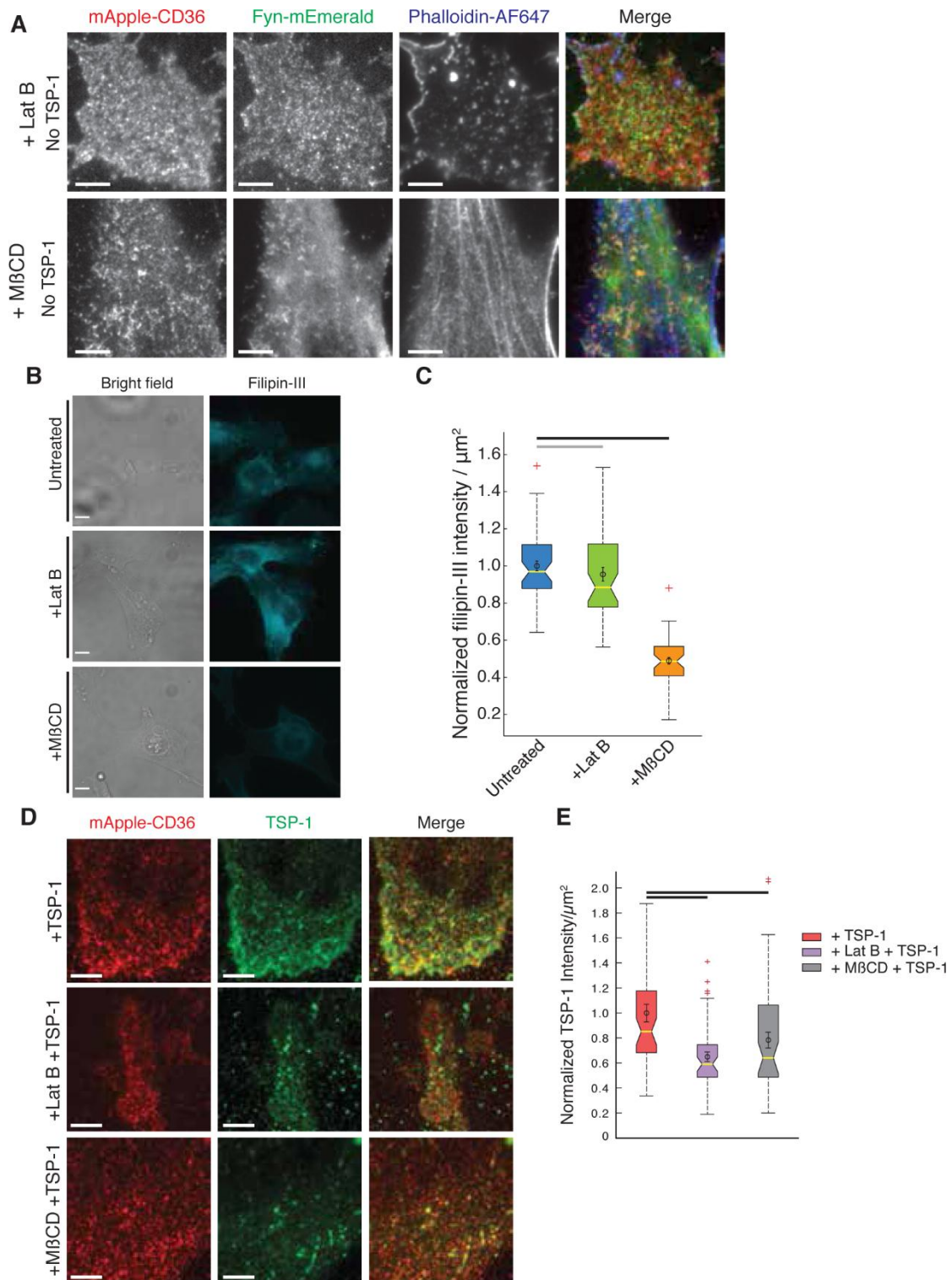


**Fig S4. Effect of actin depolymerization or cholesterol removal on CD36 and Fyn distribution and TSP-1 binding.** (A) Representative TIRFM images of mApple-CD36, Fyn-mEmerald and F-actin (Phalloidin-AlexaFluor-647) in HMEC-mApple-CD36 cells treated with LatB or M $\beta$ CD. See Fig S3A for corresponding unperturbed cells. Scale bars, 5  $\mu$ m. (B-C) Quantification of membrane cholesterol depletion during M $\beta$ CD extraction compared to untreated and LatB treated HMEC-1 cells. (B) Representative wide-field images of HMEC-1 cells treated or not with LatB or M $\beta$ CD and stained using filippin-III (Abcam). (C) Quantification of filippin-III average intensity per cell normalized to mean untreated control condition. Data from ~30 fields of view from 3 independent experiments, all imaged with identical settings. Boxplots and statistical tests as in Fig 1E (for 2 comparisons, significance threshold = 0.025 for each comparison). (D) HMEC-mApple-CD36 cells were incubated with or without LatB or M $\beta$ CD and stimulated with TSP-1 for 10 min. Bound TSP-1 was immunostained with goat anti-human TSP-1 followed by donkey anti-goat Dylight-649. Images are representative of 3 similar independent experiments, each containing at least 10 fields of view, all imaged with identical settings. (E) Quantification of the amount of TSP-1 binding to HMEC-mApple-CD36 cells in unperturbed, LatB or M $\beta$ CD treated conditions (shown in D). Boxplots and statistical tests as in Fig 1E (for 2 comparisons, significance threshold = 0.025 for each comparison).